

Regioselective Functionalization of the Mesoporous Metal–Organic Framework, NU-1000, with Photo-Active Tris-(2,2'-bipyridine)ruthenium(II)

Hisanori Nagatomi, Leighanne C. Gallington, Subhadip Goswami, Jiaxin Duan, Karena W. Chapman, Nobuhiro Yanai, Nobuo Kimizuka, Omar K. Farha, and Joseph T. Hupp*



Cite This: *ACS Omega* 2020, 5, 30299–30305



Read Online

ACCESS |



Metrics & More

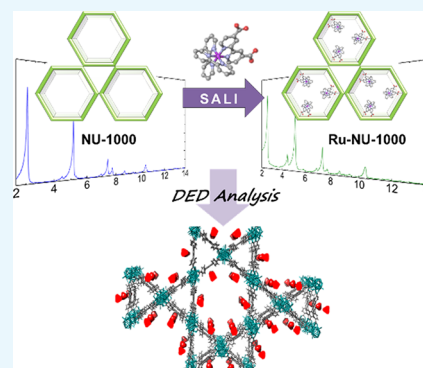


Article Recommendations



Supporting Information

ABSTRACT: Solvent-assisted ligand incorporation is an excellent method for the post-synthetic functionalization of Zr-based metal–organic frameworks (MOFs), as carboxylate-derivative functionalities readily coordinate to the Zr_6 nodes by displacing node-based aqua and terminal hydroxo ligands. In this study, a photocatalytically active ruthenium complex $Ru^{II}(bpy)_2(dcbpy)$, that is, bis-(2,2'-bipyridine)-(4,4'-dicarboxy-2,2'-bipyridine)ruthenium, was installed in the mono-protonated (carboxylic acid) form within NU-1000 *via* SALI. Crystallographic information regarding the siting of the ruthenium complex within the MOF pores is obtained by difference envelope density analysis. The ruthenium-functionalized MOF, termed Ru-NU-1000, shows excellent heterogeneous photocatalytic activity for an oxidative amine coupling reaction.



INTRODUCTION

There has been a long-standing interest in mimicking the key aspects of naturally occurring photosynthesis, that is, collecting light with artificial pigments and using the transiently captured energy to drive organic chemical transformations to store the energy in chemical bonds. Visible-light-induced chemical transformations are of particular interest due to the relatively high abundance of photons in the visible portion of the solar spectrum. Visible-light-absorbing inorganic and organometallic complexes, featuring Ru, Ir, Re, and Os, are attractive especially as potential photocatalysts for organic reactions due to the ready accessibility of long-lived triplet excited states (*via* an efficient spin–orbit-coupling facilitated intersystem crossing from initially formed singlet excited states).^{1,2} However, owing to the high cost and low abundance of these metals, catalyst recycling and reuse hold unusual appeal. To this end, heterogenizing molecular catalysts is an attractive notion, especially if the properties of the isolated molecule can be retained. Heterogenization simplifies the separation of catalysts from products, making catalyst recycling easier.

Metal–organic frameworks (MOFs) are promising scaffolds for immobilizing/heterogenizing molecular catalysts.^{3–6} Consisting of metal-ion-containing nodes and multitopic organic linkers connected by coordination bonds, MOFs offer well-defined (*i.e.*, crystalline) lattices possessing molecular-scale porosity.^{7,8} Depending on their composition, they also offer anchoring or attachment points for molecular catalysts. Notably, attachment can be accomplished after assembly of

the framework,^{9,10} thereby eliminating the need for candidate catalysts to withstand the conditions associated with MOF synthesis.¹¹ This approach is often termed post-synthetic modification (PSM). While not inclusive of every possibility, modes of PSM can be broadly classified as either elaboration of linkers^{10,12} or nodes or replacement/exchange of linkers or of metal ions comprising all or part of a node (*i.e.*, transmetallation).^{13–17}

MOFs featuring oxophilic Zr^{IV}_6 nodes are of particular interest as porous networks for various kinds of post-functionalization due to their high chemical (pH 0–10), thermal (up to 400 °C), and mechanical stability.²⁰ There are several reports of heterogenizing molecular catalysts *via* post-synthetic incorporation in Zr-MOFs. Examples include catalysts for trifluoroethylation of styrenes,²¹ carbon-dioxide reduction,^{22,23} and the aza-Henry reaction.²²

Here, we have focused on NU-1000,²⁴ $[Zr_6(\mu_3-O)_4(\mu_3-OH)_4(-OH)_4(-OH_2)_4(TBAPy)_2]$, as a support for heterogenizing molecular catalysts. (H_4TBAPy is 1,3,6,8-tetrakis(*p*-benzoic acid)pyrene; $TBAPy^{4-}$ is a tetratopic linker); and $[Zr_6(\mu_3-O)_4(\mu_3-OH)_4(-OH)_4(-OH_2)_4]^{8+}$ is the node.) The

Received: October 1, 2020

Accepted: October 29, 2020

Published: November 9, 2020



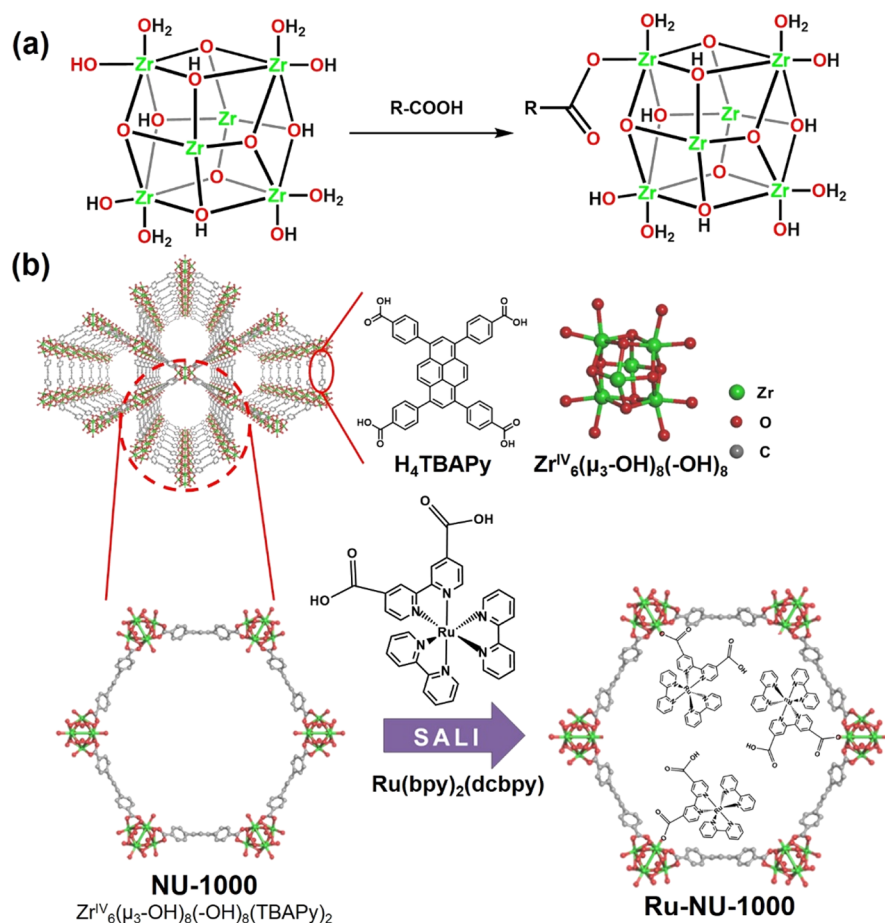


Figure 1. (a) Schematic representation of solvent-assisted ligand incorporation for nonstructural ligands that are too sterically demanding to chelate Zr.^{18,19} (b) Schematic structures of NU-1000 and its linker and Zr₆ node, together with SALI of Ru(bpy)₂(dcbpy), a nonstructural species that is sufficiently sterically demanding that node attachment is possible only *via* ester-like coordination (single carboxylate oxygen atom coordination).

MOF topology is *csq*, and the structure is illustrated in Figure 1. Notably, NU-1000 offers hierarchical mesoporosity. It also offers labile and nonstructural ligands (terminal aqua and hydroxo ligands) that can be displaced to accommodate node ligation/grafting of molecules presenting carboxylate, phosphonate, acetylacetonate, or other suitable functional groups.^{4,25,26} When carried out in solution, the grafting process is termed solvent-assisted ligand incorporation.^{25,27} A few examples of vapor-phase grafting of nonstructural ligands have also been reported.²⁶

In this study, we report the SALI-based installation of a carboxylate-derivatized ruthenium complex, Ru^{II}(bpy)₂(Hdcbpy)¹⁺, as a nonstructural ligand on the node of NU-1000 [SALI is solvent-assisted ligand incorporation, bpy is 2,2'-bipyridine, dcbpy is 4,4'-dicarboxy-2,2'-bipyridine, and H indicates that one of the two carboxylates is protonated (and not involved in node ligation)]. This example differs from the previous reports of Ru(bpy)₃²⁺-containing MOFs where incorporation of the polypyridyl complex relied either on van der Waals interactions with the walls of small pores or employed a 2,2'-bipyridine-containing linker (*i.e.* MOF structural ligand) directly as a component of the coordination sphere of Ru.^{23,28–33} X-ray structural information regarding the siting of the complex within the MOF has been obtained by difference envelope density (DED) analysis (*vide supra*). We find that the installed ruthenium complexes are chromophoric

and, when irradiated, are photocatalytically active for a representative oxidative amine coupling reaction.

EXPERIMENTAL SECTION

Materials. Acetone (Macron, 98%), acetonitrile (Macron, 99.8%), *N,N*-dimethylformamide (DMF) (Macron, 99.8%), dichloromethane (Macron, 99.0%), deuterated dimethyl sulfoxide (DMSO-*d*₆) (Cambridge Isotopes, 99%), deuterated sulfuric acid (Cambridge Isotopes, 96–98% solution in D₂O), *cis*-dichlorobis(2,2'-bipyridine)ruthenium(II) (Ru^{II}(bpy)₂Cl₂) (Sigma-Aldrich, 97%), 2,2'-bipyridine-4,4'-dicarboxylic acid (dcbpy) (Sigma-Aldrich, 98%), ammonium hexafluorophosphate (NH₄PF₆) (Aldrich), sodium bicarbonate (Aldrich), and 4-methylbenzylamine (Aldrich, 97%) were used.

Instrumentation. ¹H NMR spectra were measured on a 400 MHz Agilent DD MR-400 and a Bruker ADVANCE III 500 MHz instrument. Powder X-ray diffraction (PXRD) patterns were collected on a Rigaku ATXG (50 kV, 240 mA) and a Rigaku SmartLab (45 kV, 160 mA) instrument. Samples were scanned at a step size of 2θ = 0.02° with a 1°/min scanning speed over a range of 1.5–30°. Diffuse reflectance infrared Fourier transform spectra (DRIFTS) were recorded on a Nicolet 7600 FTIR spectrometer. The samples were prepared with KBr where KBr was used as the background. Inductively coupled plasma–optical emission spectroscopy (ICP–OES) measurements were studied on a

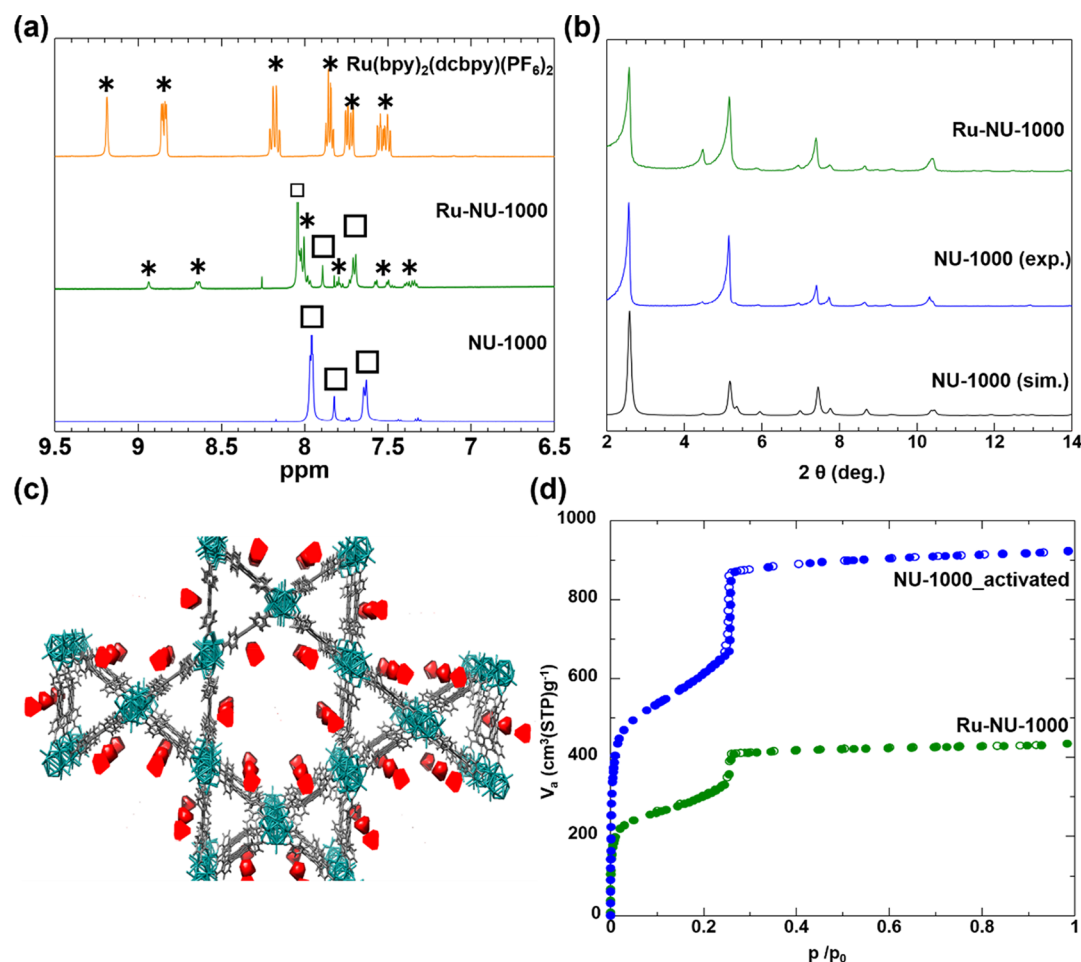


Figure 2. (a) ^1H NMR spectra of $\text{Ru}^{\text{II}}(\text{bpy})_2(\text{dcbpy})](\text{PF}_6)_2$ measured in $\text{DMSO}-d_6$, SALI-Ru-NU-1000 (green), and NU-1000 (blue) measured in $\text{D}_2\text{SO}_4/\text{DMSO}-d_6$ mixed solvent. The contributions of NU-1000 and $\text{Ru}^{\text{II}}(\text{bpy})_2(\text{dcbpy})](\text{PF}_6)_2$ in Ru-NU-1000 are shown by square boxes and *, respectively. (b) Experimental (blue) and simulated PXRD patterns of NU-1000 and SALI-Ru-NU-1000 (green). (c) DED plot showing the location of extra electron density present in SALI-Ru-NU-1000. (d) N_2 adsorption (filled circles) and desorption (open circles) isotherm curves of NU-1000 (blue) and SALI-Ru-NU-1000 (green) at 77 K. Note that each Zr node is shared by two hexagons.

Thermo iCAP 7600 ICP–OES spectrometer. MOF samples were digested in the mixture of 0.6 mL of sulfuric acid and 0.2 mL of 30% H_2O_2 and heated in a Biotage SPX microwave reactor at 150 $^\circ\text{C}$ for 5 min. This solution was then diluted with Milli-Q water to a final volume of 8 mL. Standard solutions with Zr and Ru concentrations of 10, 20, 30, and 40 ppm were used for the calibration curve. Nitrogen adsorption isotherm measurements were carried out at 77 K on a Micromeritics Tristar II 3020. Samples were activated at 120 $^\circ\text{C}$ under vacuum for 24 h prior to measuring the isotherms on a Micromeritics Smart VacPrep. Blue LED irradiation was performed by using Solderless CREE XT-E Royal Blue LEDs purchased from RapidLED which were then mounted on aluminum to give a homemade irradiation setup. The four LEDs were connected in series (power density, 325 mW/cm 2) to a Mean Well LPC-35-700 constant current driver, also purchased from RapidLED.

Synthesis and Characterization. *Synthesis of NU-1000.* NU-1000 was prepared via a solvothermal method according to the published procedure.³⁴

*Synthesis of $[\text{Ru}^{\text{II}}(\text{bpy})_2(\text{dcbpy})](\text{PF}_6)_2$ [Bis(2,2'-bipyridine)-4,4'-dicarboxy-2,2'-bipyridine ruthenium bis-(hexafluorophosphate)].*³⁵ *Cis*-dichlorobis(2,2'-bipyridine)-ruthenium(II) $[\text{Ru}^{\text{II}}(\text{bpy})_2\text{Cl}_2]$ (500 mg, 1.03 mmol), 2,2'-

bipyridine-4,4'-dicarboxylic acid (dcbpy) (302.52 mg 1.24 mmol), and sodium bicarbonate (312.2 mg, 3.72 mmol) were added to a 100 mL round-bottom flask and dissolved in the mixed solvent of water (15 mL) and methanol (10 mL). The mixture was refluxed under nitrogen for 2 h. The solution was allowed to be cooled to room temperature, and subsequently, aqueous solution of saturated ammonium hexafluorophosphate (NH_4PF_6) [504.8 mg (3.10 mmol) of NH_4PF_6 was dissolved] was added to the solution. The solution was cooled in the refrigerator overnight. After the solution was neutralized to pH 6 with diluted sulfuric acid (1 N), a red precipitate appeared. Then, the precipitate was filtered and air-dried. The obtained solid was dissolved into acetonitrile (insoluble solids were removed by filtration). By adding diethyl ether into the filtered solution, a red–orange precipitate appeared. The precipitate was filtered, washed with diethyl ether, dried, and obtained as red–black powder. The obtained powder was characterized by ^1H NMR.

Preparation of Ru-NU-1000. Activated NU-1000 (50 mg, 0.023 mmol) was soaked into 0.1 M $[\text{Ru}^{\text{II}}(\text{bpy})_2(\text{dcbpy})](\text{PF}_6)_2$ solution [217.9 mg (0.23 mmol) of $[\text{Ru}^{\text{II}}(\text{bpy})_2(\text{dcbpy})](\text{PF}_6)_2$ was dissolved into 2.3 mL of DMF] and heated at 80 $^\circ\text{C}$ for 5 days. After cooling to room temperature, the solid was filtered by the polytetrafluoro-

ethylene filter, washed with DMF until filtered liquid turned colorless, and then soaked into fresh DMF overnight. After removing DMF, the solid was soaked into fresh acetone repeatedly for solvent exchange at least three times. After removing the solvent, the solid was dried under vacuum at 100 °C. Then, Ru-NU-1000 was obtained as orange powder and characterized by DRIFTS, PXRD, DED analysis, N₂ gas adsorption, and ICP measurements.

RESULTS AND DISCUSSION

The required carboxylic-acid-derivatized tris-bipyridine ruthenium complex, [Ru^{II}(bpy)₂(H₂dcbpy)](PF₆)₂, was synthesized by following a previously reported procedure³⁵ and characterized by ¹H NMR in DMSO-*d*₆. The details of the subsequent SALI procedure are provided in the [Supporting Information](#). Briefly, activated (*i.e.*, solvent evacuated) NU-1000 was soaked in a 0.1 M solution of the [Ru^{II}(bpy)₂(H₂dcbpy)](PF₆)₂ (corresponding here to 10 equiv per Zr₆ node) in DMF at 80 °C for 5 days. The sample was then washed vigorously with DMF to remove physisorbed ruthenium complexes followed by solvent exchange with acetone. It was further thermally activated under reduced pressure to remove the solvent from the MOF pores. The Ru-complex-containing version of NU-1000, Ru-NU-1000, was obtained as orange powder. Incorporation of the ruthenium complex was confirmed by ¹H NMR after digesting SALI-treated NU-1000 in aqueous D₂SO₄ and diluting in DMSO-*d*₆ ([Figure 2a](#)). Peaks attributable to the Ru complex (as well as the MOF linker) were observed, albeit with small chemical shifts due to conversion of carboxylate groups to carboxylic acid groups by D₂SO₄. Given the low intensities of the NMR peaks, the extent of loading of the Ru complex was determined *via* ICP–OES of Ru and Zr. From these measurements, the number of Ru atoms per Zr₆ node was found to be 0.95. DRIFTS of SALI-Ru-NU-1000 shows a peak at 1230 cm^{−1} that is characteristic of C–N stretching by coordinated bipyridine and that is absent from the DRIFTS of unmodified NU-1000 ([Figure S2](#)).³⁵

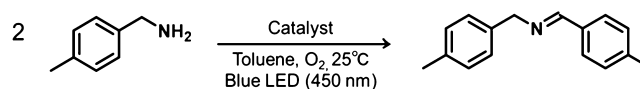
PXRD measurements of Ru-NU-1000 show that the framework is preserved after SALI-type modification ([Figure 2b](#)). Interestingly, by applying DED analysis (see [Supporting Information](#)) to PXRD data for bare NU-1000 and Ru-NU-1000,^{36,37} we find that electron density associated with the inserted Ru complexes is localized exclusively in the hexagonal pores and that it is concentrated near the tetraphenylpyrene linker. The latter observation is consistent with the known, sterically driven attachment of functionalized phenyl groups to NU-1000 *via* ester-like rather than chelating linkages.^{18,19} While the DED data show the electron density at each of the symmetry-equivalent linker faces defining the interior surface of a hexagonal pore is proximal to a node-attached ruthenium complex, that is six interior rutheniums per hexagon unit; modeling indicates that fewer than six can be spatially accommodated. A more accurate local structural interpretation is that any of six sites can be occupied, and the extent of occupancy is *ca.* 50%, that is alternating sites are occupied, as suggested in [Figure 1b](#), with the distribution sites being disordered [note that each node is shared by two hexagon units, suggesting a maximal loading (*i.e.* 50% site occupancy) of one Ru atom per node]. Modeling further suggests that occupancy alternates along the MOF *c*-axis, that is the direction in which hexagonal units are stacked. Thus, if ruthenium complexes are proximal to the first, third, and fifth

linkers defining the interior of a given hexagon, ruthenium complexes within the hexagons immediately above and below are proximal to the second, fourth, and sixth linkers. The absence of additional diffraction peaks, that would indicate a doubling of the *c*-axis of the unit cell, suggests that the Ru occupancy between adjacent channels is uncorrelated.

The porosity of the MOF was examined by performing nitrogen adsorption and desorption measurements at 77 K ([Figure 2d](#)). We observed a reduction in N₂ uptake and the Brunauer–Emmett–Teller surface area of Ru-NU-1000 (1024 m² g^{−1}) from the parent MOF NU-1000 (2131 m² g^{−1}). The lower adsorbed amount of N₂ for Ru-NU-1000 suggests that the Ru complexes were installed into the pores of NU-1000. However, the Ru-NU-1000 isotherm still exhibited type IV feature, a signature of mesoporous material suggesting the retention of the framework's original structure.

Ru-NU-1000 was evaluated as a heterogeneous photocatalyst for the aerobic oxidative amine coupling reaction.^{22,38} The reactions were carried out in toluene under O₂ and blue LED (450 nm) irradiation at room temperature with several conditions ([Table 1](#)). First of all, the molecular catalyst

Table 1. Photocatalytic Oxidative Amine Coupling with Ru-NU-1000

				
entry	catalysts ^b	time (h)	light	conversion yield ^c (%)
1 ^a	Ru(bpy) ₂ (dcbpy)(PF ₆) ₂	24	○	100
2	Ru-NU-1000	1	○	97
3	Ru-NU-1000	4	○	98
4	Ru-NU-1000 (reuse)	4	○	100
5	Ru-NU-1000	4		7
6		4	○	3
7	NU-1000	4	○	66

^aPhotocatalysis was performed in acetonitrile. ^bThe molar quantity of the catalyst was 1% that of the substrate. ^cConversion yield = 2 × [product]/([substrate] + 2 × [product]) from ¹H NMR ([Figure S4](#)). The open circles here signify irradiation.

Ru(bpy)₂(dcbpy)(PF₆)₂ was studied in acetonitrile as a control study and showed a 100% conversion within 24 h ([Table 1](#), entry 1). The MOF Ru-NU-1000 showed efficient conversion of the starting material (~97%) within an hour (Turn over number, TON ~ 100), with the yield increasing slightly after 3 additional hours (4 h total) ([Table 1](#), entries 2 and 3). These values are comparable to those reported for other MOF-based photocatalysts.^{39–41} When the reaction was performed in the absence of light, only 7% conversion of the starting material was observed, indicating the importance of irradiation for catalysis ([Table 1](#), entry 5). The reaction without Ru-NU-1000 was also evaluated under LED irradiation, but almost no conversion was observed (3%) ([Table 1](#), entry 6). The ruthenium-free parent MOF, NU-1000, accomplished 66% conversion—but only after 4 h, versus 97% conversion after 1 h for Ru-NU-1000. The slow, but substantial, conversion by ruthenium-free NU-1000 is likely due to residual absorption of blue light by tetraphenylpyrene linkers—absorption that is largely masked after ruthenium installation. When photo-excited, the linkers can sensitize the conversion of unreactive triplet (*i.e.*, ground electronic state) O₂ to reactive singlet O₂.⁴²

However, the lower extent of conversion, with unmodified NU-1000 relative to Ru-NU-1000, suggests that the high conversion (*i.e.*, nearly quantitative) with Ru-NU-1000 is due to assistance from ruthenium chromophores. The reusability of Ru-NU-1000 was also studied. After simple filtering and washing, the recovered Ru-NU-1000 was reused for the same photocatalysis and showed essentially the same degree of conversion, as observed in the initial run (Table 1 entry 4). Scanning electron microscopy–energy-dispersive X-ray spectroscopy analysis of the recovered sample shows the loading ratio of Ru/Zr6 \sim 0.8 after the reaction, suggesting retention of \sim 85% of the catalytic centers at the end of the reaction. PXRD data for the irradiated and recovered Ru-NU-1000 showed that crystallinity is retained following its use as a photocatalyst (see Figure S5).

CONCLUSIONS

A stable ruthenium-complex-containing MOF (Ru-NU-1000) can be prepared, with retention of the original framework structure, by a PSM method³⁵ and then employed as a heterogeneous photocatalyst for an aerobic oxidative amine coupling reaction. Ru-NU-1000 displays activity similar to that of the Ru complex in homogeneous solution but with the advantages of straightforward isolation from the reaction mixture and ready reusability. This work illustrates that SALI is a useful method for heterogenizing molecular photocatalysts. It also illustrates that DED analysis of X-ray diffraction data for microcrystalline powders can be used to determine the siting of molecules—in this case, photocatalysts—within MOFs featuring hierarchical porosity. Indeed, here DED data reveal selective siting within only one of three types of pores, the hexagonal mesopore. Notably, other guests, described in other studies, are selectively incorporated into either trigonal pores¹⁸ or *c*-pores,⁴³ to the exclusion of hexagonal pores. For all but the smallest guests, SALI-based anchoring appears to select primarily for the hexagonal pores.

ASSOCIATED CONTENT

Supporting Information

The Supporting Information is available free of charge at <https://pubs.acs.org/doi/10.1021/acsomega.0c04823>.

Detailed characterizations of the materials by NMR, DRIFTS, instrumentation for DED, and photocatalytic reaction (PDF)

AUTHOR INFORMATION

Corresponding Author

Joseph T. Hupp – Department of Chemistry, Northwestern University, Evanston, Illinois 60208-3113, United States; orcid.org/0000-0003-3982-9812; Email: j-hupp@northwestern.edu

Authors

Hisanori Nagatomi – Department of Chemistry, Northwestern University, Evanston, Illinois 60208-3113, United States; Department of Chemistry and Biochemistry, Graduate School of Engineering, Center for Molecular Systems (CMS), Kyushu University, Fukuoka 819-0395, Japan

Leighanne C. Gallington – X-ray Science Division, Advanced Photon Source, Argonne National Laboratory, Argonne, Illinois 60439-4858, United States; orcid.org/0000-0002-0383-7522

Subhadip Goswami – Department of Chemistry, Northwestern University, Evanston, Illinois 60208-3113, United States; orcid.org/0000-0002-8462-9054

Jiaxin Duan – Department of Chemistry, Northwestern University, Evanston, Illinois 60208-3113, United States; orcid.org/0000-0003-3252-7870

Karena W. Chapman – Department of Chemistry, Stony Brook University, Stony Brook, New York 11794-3400, United States; orcid.org/0000-0002-8725-5633

Nobuhiro Yanai – Department of Chemistry and Biochemistry, Graduate School of Engineering, Center for Molecular Systems (CMS), Kyushu University, Fukuoka 819-0395, Japan; JST-PRESTO, Kawaguchi, Saitama 332-0012, Japan; orcid.org/0000-0003-0297-6544

Nobuo Kimizuka – Department of Chemistry and Biochemistry, Graduate School of Engineering, Center for Molecular Systems (CMS), Kyushu University, Fukuoka 819-0395, Japan; orcid.org/0000-0001-8527-151X

Omar K. Farha – Department of Chemistry, Northwestern University, Evanston, Illinois 60208-3113, United States; orcid.org/0000-0002-9904-9845

Complete contact information is available at: <https://pubs.acs.org/doi/10.1021/acsomega.0c04823>

Notes

The authors declare no competing financial interest.

ACKNOWLEDGMENTS

We gratefully acknowledge support from the U.S. Dept. of Energy, Office of Science, Office of Basic Energy Sciences (grant no. DE-FG02-87ER13808) and Northwestern University. The X-ray work made use of the IMSERC at Northwestern University, which has received support from the Soft and Hybrid Nanotechnology Experimental (SHyNE) Resource (NSF NNCI-1542205), the State of Illinois, and the International Institute for Nanotechnology (IIN). The research for the DED analysis used resources of the Advanced Photon Source, a U.S. Department of Energy (DOE) Office of Science User Facility operated for the DOE Office of Science by Argonne National Laboratory under contract no. DE-AC02-06CH11357. H.N. was supported by the Leading Graduate School for Advanced Graduate Course on Molecular Systems for Devices of Kyushu University by MEXT (Ministry of Education, Culture, Sports, Science and Technology).

REFERENCES

- (1) Schultz, D. M.; Yoon, T. P. Solar Synthesis: Prospects in Visible Light Photocatalysis. *Science* **2014**, *343*, 1239176.
- (2) Yoon, T. P.; Ischay, M. A.; Du, J. Visible light photocatalysis as a greener approach to photochemical synthesis. *Nat. Chem.* **2010**, *2*, 527–532.
- (3) Rimoldi, M.; Nakamura, A.; Vermeulen, N. A.; Henkelis, J. J.; Blackburn, A. K.; Hupp, J. T.; Stoddart, J. F.; Farha, O. K. A metal–organic framework immobilised iridium pincer complex. *Chem. Sci.* **2016**, *7*, 4980–4984.
- (4) Madrahimov, S. T.; Gallagher, J. R.; Zhang, G.; Meinhart, Z.; Garibay, S. J.; Delferro, M.; Miller, J. T.; Farha, O. K.; Hupp, J. T.; Nguyen, S. T. Gas-Phase Dimerization of Ethylene under Mild Conditions Catalyzed by MOF Materials Containing (bpy)NiII Complexes. *ACS Catal.* **2015**, *5*, 6713–6718.
- (5) Wu, C.-D.; Zhao, M. Incorporation of Molecular Catalysts in Metal–Organic Frameworks for Highly Efficient Heterogeneous Catalysis. *Adv. Mater.* **2017**, *29*, 1605446.

- (6) Li, Z.; Rayder, T. M.; Luo, L.; Byers, J. A.; Tsung, C.-K. Aperture-Opening Encapsulation of a Transition Metal Catalyst in a Metal–Organic Framework for CO₂ Hydrogenation. *J. Am. Chem. Soc.* **2018**, *140*, 8082–8085.
- (7) Kitagawa, S.; Kitaura, R.; Noro, S.-i. Functional Porous Coordination Polymers. *Angew. Chem., Int. Ed.* **2004**, *43*, 2334–2375.
- (8) Furukawa, H.; Cordova, K. E.; O’Keeffe, M.; Yaghi, O. M. The Chemistry and Applications of Metal–Organic Frameworks. *Science* **2013**, *341*, 1230444.
- (9) Islamoglu, T.; Goswami, S.; Li, Z.; Howarth, A. J.; Farha, O. K.; Hupp, J. T. Postsynthetic Tuning of Metal–Organic Frameworks for Targeted Applications. *Acc. Chem. Res.* **2017**, *50*, 805–813.
- (10) Cohen, S. M. Postsynthetic Methods for the Functionalization of Metal–Organic Frameworks. *Chem. Rev.* **2012**, *112*, 970–1000.
- (11) Falcaro, P.; Ricco, R.; Doherty, C. M.; Liang, K.; Hill, A. J.; Styles, M. J. MOF positioning technology and device fabrication. *Chem. Soc. Rev.* **2014**, *43*, 5513–5560.
- (12) Nguyen, H. G. T.; Weston, M. H.; Sarjeant, A. A.; Gardner, D. M.; An, Z.; Carmieli, R.; Wasielewski, M. R.; Farha, O. K.; Hupp, J. T.; Nguyen, S. T. Design, Synthesis, Characterization, and Catalytic Properties of a Large-Pore Metal–Organic Framework Possessing Single-Site Vanadyl(monocatecholate) Moieties. *Cryst. Growth Des.* **2013**, *13*, 3528–3534.
- (13) Xu, Y.; Vermeulen, N. A.; Liu, Y.; Hupp, J. T.; Farha, O. K. SALE-Ing a MOF-Based “Ship of Theseus.” Sequential Building-Block Replacement for Complete Reformulation of a Pillared-Paddlewheel Metal–Organic Framework. *Eur. J. Inorg. Chem.* **2016**, 4345–4348.
- (14) Karagiari, O.; Bury, W.; Mondloch, J. E.; Hupp, J. T.; Farha, O. K. Solvent-Assisted Linker Exchange: An Alternative to the De Novo Synthesis of Unattainable Metal–Organic Frameworks. *Angew. Chem., Int. Ed.* **2014**, *53*, 4530–4540.
- (15) Pullen, S.; Fei, H.; Orthaber, A.; Cohen, S. M.; Ott, S. Enhanced Photochemical Hydrogen Production by a Molecular Diiron Catalyst Incorporated into a Metal–Organic Framework. *J. Am. Chem. Soc.* **2013**, *135*, 16997–17003.
- (16) Deria, P.; Mondloch, J. E.; Karagiari, O.; Bury, W.; Hupp, J. T.; Farha, O. K. Beyond post-synthesis modification: evolution of metal–organic frameworks via building block replacement. *Chem. Soc. Rev.* **2014**, *43*, 5896–5912.
- (17) Takaishi, S.; DeMarco, E. J.; Pellin, M. J.; Farha, O. K.; Hupp, J. T. Solvent-assisted linker exchange (SALE) and post-assembly metallation in porphyrinic metal–organic framework materials. *Chem. Sci.* **2013**, *4*, 1509–1513.
- (18) Goswami, S.; Noh, H.; Redfern, L. R.; Otake, K.-i.; Kung, C.-W.; Cui, Y.; Chapman, K. W.; Farha, O. K.; Hupp, J. T. Pore-Templated Growth of Catalytically Active Gold Nanoparticles within a Metal–Organic Framework. *Chem. Mater.* **2019**, *31*, 1485–1490.
- (19) Liu, J.; Li, Z.; Zhang, X.; Otake, K.-i.; Zhang, L.; Peters, A. W.; Young, M. J.; Bedford, N. M.; Letourneau, S. P.; Mandia, D. J.; Elam, J. W.; Farha, O. K.; Hupp, J. T. Introducing Nonstructural Ligands to Zirconia-like Metal–Organic Framework Nodes To Tune the Activity of Node-Supported Nickel Catalysts for Ethylene Hydrogenation. *ACS Catal.* **2019**, *9*, 3198–3207.
- (20) Howarth, A. J.; Liu, Y.; Li, P.; Li, Z.; Wang, T. C.; Hupp, J. T.; Farha, O. K. Chemical, thermal and mechanical stabilities of metal–organic frameworks. *Nat. Rev. Mater.* **2016**, *1*, 15018.
- (21) Yu, X.; Cohen, S. M. Photocatalytic Metal–Organic Frameworks for Selective 2,2,2-Trifluoroethylation of Styrenes. *J. Am. Chem. Soc.* **2016**, *138*, 12320–12323.
- (22) Wang, C.; Xie, Z.; deKrafft, K. E.; Lin, W. Doping Metal–Organic Frameworks for Water Oxidation, Carbon Dioxide Reduction, and Organic Photocatalysis. *J. Am. Chem. Soc.* **2011**, *133*, 13445–13454.
- (23) Kajiwara, T.; Fujii, M.; Tsujimoto, M.; Kobayashi, K.; Higuchi, M.; Tanaka, K.; Kitagawa, S. Photochemical Reduction of Low Concentrations of CO₂ in a Porous Coordination Polymer with a Ruthenium(II)–CO Complex. *Angew. Chem., Int. Ed.* **2016**, *55*, 2697–2700.
- (24) Mondloch, J. E.; Katz, M. J.; Planas, N.; Semrouni, D.; Gagliardi, L.; Hupp, J. T.; Farha, O. K. Are Zr₆-based MOFs water stable? Linker hydrolysis vs. capillary-force-driven channel collapse. *Chem. Commun.* **2014**, *50*, 8944–8946.
- (25) Deria, P.; Bury, W.; Hupp, J. T.; Farha, O. K. Versatile functionalization of the NU-1000 platform by solvent-assisted ligand incorporation. *Chem. Commun.* **2014**, *50*, 1965–1968.
- (26) Liu, J.; Ye, J.; Li, Z.; Otake, K.-i.; Liao, Y.; Peters, A. W.; Noh, H.; Truhlar, D. G.; Gagliardi, L.; Cramer, C. J.; Farha, O. K.; Hupp, J. T. Beyond the Active Site: Tuning the Activity and Selectivity of a Metal–Organic Framework-Supported Ni Catalyst for Ethylene Dimerization. *J. Am. Chem. Soc.* **2018**, *140*, 11174–11178.
- (27) Deria, P.; Mondloch, J. E.; Tylanakis, E.; Ghosh, P.; Bury, W.; Snurr, R. Q.; Hupp, J. T.; Farha, O. K. Perfluoroalkane Functionalization of NU-1000 via Solvent-Assisted Ligand Incorporation: Synthesis and CO₂ Adsorption Studies. *J. Am. Chem. Soc.* **2013**, *135*, 16801–16804.
- (28) Isaka, Y.; Kondo, Y.; Kuwahara, Y.; Mori, K.; Yamashita, H. Incorporation of a Ru complex into an amine-functionalized metal–organic framework for enhanced activity in photocatalytic aerobic benzyl alcohol oxidation. *Catal. Sci. Technol.* **2019**, *9*, 1511–1517.
- (29) Qin, X.; Zhang, X.; Wang, M.; Dong, Y.; Liu, J.; Zhu, Z.; Li, M.; Yang, D.; Shao, Y. Fabrication of Tris(bipyridine)ruthenium(II)-Functionalized Metal–Organic Framework Thin Films by Electrochemically Assisted Self-Assembly Technique for Electrochemiluminescent Immunoassay. *Anal. Chem.* **2018**, *90*, 11622–11628.
- (30) Yang, H.; Fei, H. A generic and facile strategy to fabricate metal–organic framework films on TiO₂ substrates for photocatalysis. *Dalton Trans.* **2017**, *46*, 2751–2755.
- (31) Maza, W. A.; Haring, A. J.; Ahrenholtz, S. R.; Epley, C. C.; Lin, S. Y.; Morris, A. J. Ruthenium(ii)-polypyridyl zirconium(iv) metal–organic frameworks as a new class of sensitized solar cells. *Chem. Sci.* **2016**, *7*, 719–727.
- (32) Wang, X.; Lu, W.; Gu, Z.-Y.; Wei, Z.; Zhou, H.-C. Topology-guided design of an anionic bor-network for photocatalytic [Ru(bpy)₃]²⁺ encapsulation. *Chem. Commun.* **2016**, *52*, 1926–1929.
- (33) Yu, X.; Cohen, S. M. Photocatalytic metal–organic frameworks for the aerobic oxidation of arylboronic acids. *Chem. Commun.* **2015**, *51*, 9880–9883.
- (34) Wang, T. C.; Vermeulen, N. A.; Kim, I. S.; Martinson, A. B. F.; Stoddart, J. F.; Hupp, J. T.; Farha, O. K. Scalable synthesis and post-modification of a mesoporous metal–organic framework called NU-1000. *Nat. Protoc.* **2016**, *11*, 149–162.
- (35) Rasalingam, S.; Peng, R.; Wu, C.-M.; Mariappan, K.; Koodali, R. T. Robust and effective Ru-bipyridyl dye sensitized Ti-MCM-48 cubic mesoporous materials for photocatalytic hydrogen evolution under visible light illumination. *Catal. Commun.* **2015**, *65*, 14–19.
- (36) Yakovenko, A. A.; Reibenspies, J. H.; Bhuvanesh, N.; Zhou, H.-C. Generation and applications of structure envelopes for porous metal–organic frameworks. *J. Appl. Crystallogr.* **2013**, *46*, 346–353.
- (37) Yakovenko, A. A.; Wei, Z.; Wriedt, M.; Li, J.-R.; Halder, G. J.; Zhou, H.-C. Study of Guest Molecules in Metal–Organic Frameworks by Powder X-ray Diffraction: Analysis of Difference Envelope Density. *Cryst. Growth Des.* **2014**, *14*, 5397–5407.
- (38) Ko, J. H.; Kang, N.; Park, N.; Shin, H.-W.; Kang, S.; Lee, S. M.; Kim, H. J.; Ahn, T. K.; Son, S. U. Hollow Microporous Organic Networks Bearing Triphenylamines and Anthraquinones: Diffusion Pathway Effect in Visible Light-Driven Oxidative Coupling of Benzylamines. *ACS Macro Lett.* **2015**, *4*, 669–672.
- (39) Xu, C.; Liu, H.; Li, D.; Su, J.-H.; Jiang, H.-L. Direct evidence of charge separation in a metal–organic framework: efficient and selective photocatalytic oxidative coupling of amines via charge and energy transfer. *Chem. Sci.* **2018**, *9*, 3152–3158.
- (40) Chen, P.; Guo, Z.; Liu, X.; Lv, H.; Che, Y.; Bai, R.; Chi, Y.; Xing, H. A visible-light-responsive metal–organic framework for highly efficient and selective photocatalytic oxidation of amines and reduction of nitroaromatics. *J. Mater. Chem. A* **2019**, *7*, 27074–27080.

- (41) Yang, X.; Huang, T.; Gao, S.; Cao, R. Boosting photocatalytic oxidative coupling of amines by a Ru-complex-sensitized metal-organic framework. *J. Catal.* **2019**, *378*, 248–255.
- (42) Liu, Y.; Buru, C. T.; Howarth, A. J.; Mahle, J. J.; Buchanan, J. H.; DeCoste, J. B.; Hupp, J. T.; Farha, O. K. Efficient and selective oxidation of sulfur mustard using singlet oxygen generated by a pyrene-based metal–organic framework. *J. Mater. Chem. A* **2016**, *4*, 13809–13813.
- (43) Peters, A. W.; Otake, K.; Platero-Prats, A. E.; Li, Z.; DeStefano, M. R.; Chapman, K. W.; Farha, O. K.; Hupp, J. T. Site-Directed Synthesis of Cobalt Oxide Clusters in a Metal–Organic Framework. *ACS Appl. Mater. Interfaces* **2018**, *10*, 15073–15078.